Research Article

Visual response characteristics of neurons in the second visual area of marmosets

Yin Yang[1, 2, #], Ke Chen[3, #], Marcello G. P. Rosa[4], Hsin-Hao Yu[4], Li-Rong Kuang[5], Jie Yang[2, 6, *]

Graphical Abstract *Area V2 plays an important role in locating objects in space and detecting the direction of motion of objects*
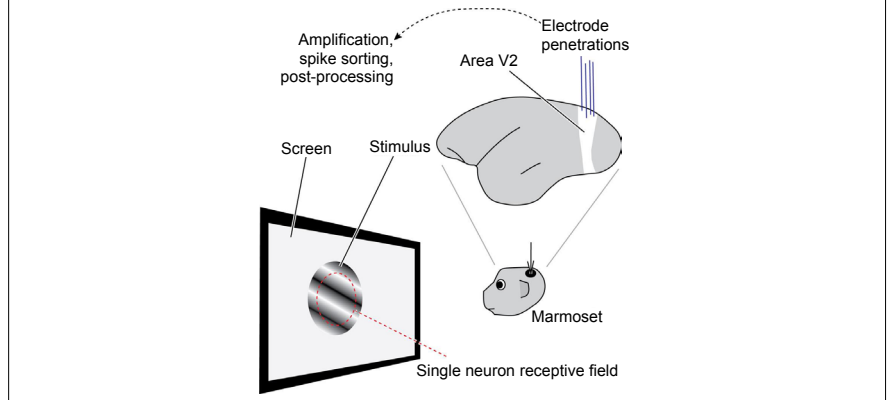
Abstract

The physiological characteristics of the marmoset second visual area (V2) are poorly understood compared with those of the primary visual area (V1). In this study, we observed the physiological response characteristics of V2 neurons in four healthy adult marmosets using intracortical tungsten microelectrodes. We recorded 110 neurons in area V2, with receptive fields located between 8° and 15° eccentricity. Most (88.2%) of these neurons were orientation selective, with half-bandwidths typically ranging between 10° and 30°. A significant proportion of neurons (28.2%) with direction selectivity had a direction index greater than 0.5. The vast majority of V2 neurons had separable spatial frequency and temporal frequency curves and, according to this criterion, they were not speed selective. The basic functional response characteristics of neurons in area V2 resemble those found in area V1. Our findings show that area V2 together with V1 are important in primate visual processing, especially in locating objects in space and in detecting an object's direction of motion. The methods used in this study were approved by the Monash University Animal Ethics Committee, Australia (MARP 2009-2011) in 2009.
Key Words: direction selectivity; electrophysiological recording; marmoset; orientation selectivity; receptive field; second visual area; spatial frequency; speed selectivity; temporal frequency

Chinese Library Classification No. R445; R339.14+6; S865.1+6

Introduction

In primates, the visual cortex includes the primary visual area (striate cortex, V1) and multiple extrastriate areas. The second visual area (V2) is the largest component of the primate extrastriate cortex (Rosa et al., 1988; Sereno et al., 1995; Olavarria and Van Essen, 1997). Usually, V2 receives visual stimulation from V1 and then transmits processed information through axonal connections to other visual areas (Cowey, 1964; Zeki, 1971; Girard and Bullier, 1989). At the same time, the results of computations occurring in V2 can also be transmitted to V1 in a feedback manner (Nurminen et al., 2018). Collectively, receptive fields of V2 neurons form a complete representation of the visual field, distinct from that in V1 (Gattass et al., 1981; Rosa et al., 1997).

Marmoset monkeys are among the smallest primates and are increasingly used for studies of visual processing (Solomon and Rosa, 2014; Liu et al., 2020; Majka et al., 2020). Compared with V1, the physiological characteristics of V2 have been the subject of relatively few studies in the marmoset (Rosa et al., 1997; Lui et al., 2005; Barraclough et al., 2006; Valverde Salzmann et al., 2012).

[1]Department of Ophthalmology, Sichuan Academy of Medical Sciences & Sichuan Provincial People's Hospital, Chengdu, Sichuan Province, China; [2]College of Medicine, University of Electronic Science and Technology of China, Chengdu, Sichuan Province, China; [3]School of Life Science and Technology, University of Electronic Science and Technology of China, Chengdu, Sichuan Province, China; [4]Department of Physiology, Monash University, Melbourne, VIC, Australia; [5]Chengdu Medical College, Chengdu, Sichuan Province, China; [6]Department of Neurology, Sichuan Academy of Medical Sciences & Sichuan Provincial People's Hospital, Chengdu, Sichuan Province, China.
*Correspondence to: Jie Yang, MS, yjsh303303@126.com.
https://orcid.org/0000-0002-6833-2680 (Jie Yang)
#Both authors contributed equally to this work.

Research Article

In this study, we analyzed the neuronal response characteristics of marmoset V2 using sine wave grating stimuli, and compared them with the characteristics of V1 neurons. In particular, we addressed the question of whether V2 neurons have separable, or interacting spatial and temporal frequency (SF and TF) selectivity, which is relevant for understanding how neurons in the cortex compute the true speed of moving patterns (Priebe et al., 2003). In the marmoset the proportion of speed-selective neurons is lower in V1 compared with extrastriate area MT (middle temporal area) (Lui et al., 2007; Yu et al., 2010), but it is unknown whether V2 contains such speed-selective neurons. This article explores this possibility.

Materials and Methods

Experimental animals
Data were obtained from four healthy adult marmosets (three males and one female) aged between 1 year and 187 days to 2 years and 15 days, and weighing between 346–381 g. The animals were obtained from Australia's National Non-Human Primate Facility and the experimental procedures were approved by the Monash University Animal Ethics Committee, Australia (MARP 2009-2011) in 2019.

Animal preparation
The surgical procedures employed have been explained in detail (Bourne and Rosa 2003; Yu and Rosa 2010). In brief, following premedication with diazepam (5 mg/kg) and atropine (0.2 mg/kg; Troy Laboratories, Glendenning, Australia), anesthesia was induced by intramuscular injection of Alfaxan (alfaxalone, 10 mg/kg; Jurox, Rutherford, Australia). Following surgery, the animals were anesthetized by an intravenous infusion of sufentanil (6 μg/kg per hour; Janssen P/L Macquarie Park, Australia) and artificially ventilated with a gaseous mixture of nitrous oxide and oxygen (70:30). Neuromuscular block was achieved by intravenous injection of pancuronium bromide (0.1 mg/kg per hour; Astra Zeneca, North Ryde, Australia). An electrocardiogram and the oxygen saturation level were continuously monitored. Appropriate focus and protection of the cornea from desiccation were achieved by means of contact lenses. These lenses brought into focus the surface of a calibrated cathode ray tube monitor (Multiscan G520, 100 Hz refresh rate; Sony, Minato, Tokyo) located 60 cm away from the animal. Visual stimuli were monocularly presented to the eye contralateral to the cortical hemisphere from which the neuronal recordings were obtained. The ipsilateral eye was occluded. A craniotomy was performed to expose the dorsal surface of area V2, based on its expected stereotaxic coordinates (Rosa et al., 1997; Paxinos et al., 2012).

Electrophysiological recordings
Parylene-coated tungsten microelectrodes (~1 MΩ, WE3001XXF; MicroProbe, Fremont, CA, USA) with exposed tips of 10 μm were used. An electrode was slowly advanced into the cortex through a small slit in the dura mater, until the first units could be observed above background activity. To avoid recording instability caused by brain pulsation, the craniotomy was covered with a 2–4-mm-thick layer of warm agar (2%), as well as melted bone wax if deemed necessary. Amplification and filtering (bandpass 300 Hz–5 kHz) of electrophysiological signals were achieved using a Model 1800 microelectrode AC amplifier (AM Systems, Everett, WA, USA) and a 50-Hz line noise filter (HumBug; Quest Scientific, Vancouver, Canada). The data were collected using Expo software (designed by Peter Lennie, New York University), which also allows for online spike discrimination.

Quantitative analysis
Once the electrode was positioned in a new location (typically after 100–200 μm of vertical movement), the action potentials corresponding to the most prominent unit were isolated, and the boundaries of minimum response receptive fields of the corresponding neuron were mapped using stimuli moved on the surface of the screen. The Expo software system was then used to generate stimuli consisting of drifting sine-wave gratings (66% contrast) centered on the same location. The characteristics of the grating pattern were varied in orientation, SF and drifting speed (Yu et al., 2010). Each condition (i.e. a combination of orientation, SF and TF) was repeated eight times, with each stimulus lasting for 2 seconds.

Brain histopathology
At the end of the experiments the animals were administered an overdose of sodium pentobarbitone (Lethabarb, Virbac, Milperra, Australia) and perfused transcardially with 0.9% saline, followed by 4% paraformaldehyde in 0.1 M phosphate buffer (pH 7.4). After cryoprotection using increasing concentrations of sucrose, and sectioning, alternate slides (40 μm) were stained for Nissl substance and cytochrome oxidase using protocols optimized for marmoset brain tissue (Worthy and Burman, 2017; Worthy and Rosa, 2017). These sections were used for reconstruction of electrode tracks relative to histological borders. The electrode tracks were reconstructed with the aid of small electrolytic lesions (4 μA, 10 seconds), which were placed at various sites during the experiments.

Data analysis
We used circular variance to quantify orientation selectivity. For this calculation, $R(\theta_j)$ denotes the above-spontaneous firing rate of a neuron's response to a grating drifting at direction θ_j ($0° \leq \theta_j < 360°$, j = 0, 1, ... n). Circular variance is defined as

$$1 - \frac{\left| \sum_{j=0}^{n} R(\theta_j)\, e^{-2*i*\theta_j} \right|}{\sum_{j=0}^{n} R(\theta_j)}$$

$0 \leq$ circular variance ≤ 1. When circular variance was ≥ 0.9, the neuron was regarded as non-orientation selective; when circular variance was < 0.9, the neuron was regarded as orientation selective.

As a second measure of orientation tuning we used the half-width-half-height (HWHH) bandwidth, which is a common measure of the narrowness of orientation tuning (Campbell et al., 1968; Rose and Blakemore, 1974). The HWHH is the deviation from the optimal orientation such that the response rate of the neuron becomes half of the maximum value; thus, the smaller the HWHH bandwidth value, the greater the degree of orientation selectivity.

We also calculated the direction index (DI2pt) as a measure of direction selectivity (Schiller et al., 1976). The DI2pt was calculated as (Ori.a − Ori.b)/Ori.a, where Ori.a is the orientation of the grating to which the neuron had the maximum response, and Ori.b = Ori.a ± 180°. The DI2pt varied between 0 and 1; a neuron was regarded as direction selective when DI2pt > 0.5, and as non-direction selective when DI2pt ≤ 0.5.

The Q value (Yu et al., 2010) characterizes the degree to which the optimal TF of a neuron varies with SF. As speed is the ratio of TF to SF, Q also characterizes the degree to which the optimal speed of the neuron is invariant to the SF. A neuron with perfectly separable SF and TF tuning has $Q = 0$, and a perfectly speed-tuned neuron has $Q = 1$. Previous work has indicated that Q varies continuously in area V1, with most neurons showing intermediate values (Yu et al., 2010). In this study, neurons were regarded as speed selective when $Q \geq 0.8$, reflecting earlier findings in area MT (Lui et al., 2007).

Results

Sample characteristics
Twenty-seven electrode penetrations were completed in four

marmosets. Sixteen were confirmed to be entirely located in area V2 based on histological reconstruction (**Figure 1**). The 130 neurons recorded in these tracks had receptive fields centered between 8° and 15° in the lower visual field, covering all polar angles between the horizontal and vertical meridians, as expected from previous studies (Rosa et al., 1997). After removing 20 neurons for which response levels were too low to allow fitting of tuning curves, 110 neurons were ultimately included in the analysis.

Orientation and direction selectivity of neurons in the second visual area

Examples of tuning curves for two different neurons are illustrated in **Figure 2**. The neuronal responses shown in **Figure 2A** are representative of a direction-tuned cell (DI2pt > 0.5) whereas those shown in **Figure 2B** show orientation selectivity, but did not fit the criterion for direction selectivity.

According to a circular variance criterion of < 0.9, 97 of the 110 neurons studied (88.2%) had orientation selectivity. The HWHH bandwidth in this sample varied between 11.77°–69.1°, with a median value of 19.65° (**Figure 3A**).

The distribution of direction indices (DI2pt) is illustrated in **Figure 3B**. According to a criterion of DI2pt > 0.5, 31 neurons (28.2%) had direction selectivity (e.g. **Figure 2A**). Among these neurons the average DI2pt was 0.72. No bias for specific ranges of directions was observed, with neurons showing preferences throughout the possible range (1°–359°) in approximately equal amounts.

Optimal SF and TF of neurons in the second visual area

Figure 3C shows the distribution of optimal SF for the 110 neurons in the sample, which, as described above, were centered in mid-peripheral eccentricities (8–15°). The minimum optimal SF value was 0.02 cycles per degree (c/°), and the maximum value was 2.0 c/°. The median value was 0.45 c/°, with the majority (*n* = 85, 77.3%) of neurons exhibiting values below 0.8 c/°.

The optimal TF in the same group of neurons ranged between 0.5 Hz and 13.8 Hz, with a median value of 2.83 Hz (**Figure 3D**). A large majority of neurons (*n* = 97, 88.2%) had optimal TF values below 6 Hz.

Interaction between SF and TF selectivity (Q values) of neurons in the second visual area

The *Q* value of most neurons (*n* = 72) was not significantly different from 0, indicating that the TF of the stimuli did not affect SF selectivity. We also investigated whether the sub-population of neurons with direction selectivity (*n* = 31) tended to show interaction between SF and TF. As shown in **Figure 3E**, the average *Q* value among this population was 0.37, compatible with a mild interaction. No neuron showed a *Q* value above 0.8, which in previous studies has been associated with speed selectivity (Lui et al., 2007; Yu et al., 2010). Thus, V2 neurons did not show the physiological characteristics associated with speed selectivity.

Optimal speeds of neurons in the second visual area

Figure 3F illustrates the distribution of optimal speeds in the sample (*n* = 110), calculated using the equation, speed = TF/SF (Yu et al., 2010). The minimum optimal speed was 0.76°/s, the maximum 153.81°/s, and the median value was 9.14°/s.

Discussion

We have characterized the response selectivity of 110 neurons in marmoset area V2. Using sine wave gratings as stimuli, we explored the selectivity to orientation, direction of motion, SF, TF and speed.

Orientation selectivity

In our study, 88.2% of neurons showed clear orientation selectivity; responses above background activity required sine wave stimulation with orientation within an optimal range. This result is similar to those from studies of area V1 in different species, where most of the neurons in the visual cortex showed high selectivity for the orientation of lines, edges and gratings (e.g. Hubel and Wiesel, 1959, 1962, 1968; Henry et al., 1973; Watkins and Berkley, 1974; De Valois et al., 1982; Ringach et al., 2002; Yu and Rosa, 2014). In marmoset V2, Lui et al. (2005) reported that 73.3% of neurons were selective to orientation, using moving bars as stimuli. In the macaque, the proportion of orientation-selective or orientation-biased neurons in V2 was estimated as 72% in a study that used sine wave gratings similar to the ones employed here (Levitt et al., 1994).

We used the HWHH bandwidth to evaluate the sharpness of orientation tuning. We found a wide range of HWHH bandwidth values in the 110 V2 neurons measured, with a minimum value of 11.77° and a maximum value of 100.06°. Using similar stimuli (sine wave gratings) of macaque area V1, De Valois et al. (1982) reported an average value of 21.0° for the HWHH bandwidth of neurons with a receptive field in the paracentral representation, whereas values obtained for similar stimuli in marmoset V1 ranged between 22.1° (Sengpiel et al., 1996) and 29° (Yu and Rosa, 2014). These values are comparable to the present observations in V2 (median = 19.7°; mean = 23.9°). Similarly, Levitt et al. (1994) reported a median HWHH bandwidth value of 28.8° in the central representation of macaque V2, which they regarded as similar to that found in V1 of the same species. Comparisons with other studies of primate V2 (e.g. Baizer et al., 1977; Zeki, 1978; Orban et al., 1985) are difficult because of the wide variety of methodologies used, including awake versus anaesthetized preparations, criteria used to assign orientation selectivity, and types of stimuli, all of which are likely to influence the estimates of proportions of orientation selective neurons and precision of tuning (Rosa et al., 1992). Unlike in the dorsomedial area (DM) of the marmoset (Lui et al., 2006), there was no evidence of a bimodal distribution of orientation indices, which could point to different functional classes of neuron.

In humans, visual neurons are most sensitive to stimuli that move in vertical or horizontal planes; this is also observed in rhesus monkeys (Campbell and Kulikowski, 1966; Mitchell et al., 1967; Kawabe, 2012; Patten et al., 2017; He et al., 2020). Studies by Mansfield et al. and others (Mansfield, 1974; Mansfield and Ronner, 1978; De Valois et al., 1982; Tao et al., 2012) revealed bias towards horizontal or vertical orientations among neurons with receptive fields corresponding to foveal vision, but not among those representing paracentral vision. Similar to previous findings in marmoset V1 (Yu and Rosa, 2014), we observed no such bias among the 97 orientation-selective V2 neurons representing near-peripheral vision.

Direction selectivity

Using the direction index as a measure, we found that over a quarter of V2 neurons (28.2%) showed significant direction selectivity. This value was higher than that reported using the same metric in the corresponding region of marmoset V1 (representation of the near periphery; 21.4%) by Yu and Rosa (2014), and in area DM by Lui et al. (2006). However, studies in macaque V1 have reported similar proportions of direction selective neurons using the same type of stimulus (sine wave gratings) and criterion (DI2pt > 0.5; 29%, De Valois et al., 1982; 23%, Gur et al., 2005). Estimates of the proportion of direction selective neurons in macaque area V2, also using sine wave gratings, ranged between 15% (Levitt et al., 1994) and 38% (Foster et al., 1985). In marmoset, Lui et al. (2005) reported that 8 of 45 cells (17.8%) were direction selective to

moving bars presented against a dynamic texture background. In anaesthetized cat, Hubel and Wiesel (1962) reported that 29% of V1 neurons had direction selectivity, a value that closely matches our estimates for marmoset V2. In addition, Carandini and Ferster (2000) reported a mean direction index of 0.79 for 41 neurons in cat V1, which is also consistent with the present findings.

Optimal SF
Human visual acuity decreases markedly from central foveal vision towards peripheral vision (Virsu and Rovamo, 1979; Banks et al., 1991; Yu et al., 2015). Correspondingly, Yu et al. (2010) found that the SFs of the gratings capable of eliciting maximal responses in V1 neurons decrease significantly with increasing receptive field eccentricity. Specifically, the average optimal SF of neurons with receptive fields in central vision (3°–5°) was 1.08 c/°, whereas for neurons representing paracentral (8°–15°) and far peripheral (50°–70°) visual fields the average optimal SF became gradually lower (0.48 c/° and 0.14 c/°, respectively).

In our study, the average optimal SF of V2 neurons with receptive fields in the paracentral visual field (8°–15°) was 0.52 c/°. This result is similar to that in the corresponding part of V1, supporting the view that the optimal SF scales with the eccentricity of receptive fields in both areas (Schiller and Malpeli, 1977; Movshon et al., 1978; Xu et al., 2007; Henriksson et al., 2008; Naito et al., 2013; Zhao et al., 2016). However, neurons in areas DM and MT have preferences for lower SFs in comparison with V1 and V2 (Lui et al., 2006, 2007). In macaque V2, the range of optimal SF of neurons in central vision (2°–5°) varied between 0.2–2.1 c/° (Foster et al., 1985). In cat, high-SF-tuned surround suppression in V1 has also been observed, which caused the SF tuning to shift towards lower values when large stimuli were used (Osaki et al., 2011). In the present study, the stimuli were adjusted to cover the classical receptive field and not invade the surround, based on a size summation test (Yu and Rosa, 2014).

Optimal TF and possible selectivity to speed
In humans, the optimal TFs of visual stimuli at different eccentricities are similar (Virsu et al., 1982; Kelly, 1984; Snowden and Hess, 1992). This suggests that the optimal TF of cortical neurons does not vary markedly with eccentricity. Indeed, in marmoset V1 the average optimal TFs of neurons with receptive fields in the central, paracentral and peripheral visual fields proved to be similar (3.7 Hz, 3.0 Hz and 4.0 Hz, respectively (Yu et al., 2010). In our study, the optimal TF of neurons in the paracentral representation of area V2 was 3.5 Hz, which was similar to the above findings, and also very similar to the findings of Foster et al. (1985) in macaque V1 and V2 (3.7 and 3.5 Hz, respectively).

In macaques, the TF tuning curve of some neurons in V2 changes with the SF of the grating stimulus, but not to a sufficient degree to enable speed-invariant coding (Foster et al., 1985). The same study found no evidence of this in V1 neurons, indicating independent coding of SF and TF, as also suggested by Tolhurst and Movshon (1975). Our findings in the marmoset support the view that some V2 neurons show interactions between SF and TF tuning, but true (SF-independent) speed selectivity is absent or very rare. The proportion of such neurons is relatively increased in area MT (Priebe et al., 2003; Lui et al., 2007).

A related question is whether V2 neurons show speed selectivity to natural stimuli, which, unlike sine wave gratings, are composed of multiple SFs. In general, the peripheral visual field of primates is sensitive to stimulus images of high speed (Eckert and Buchsbaum, 1993). In the visual cortex of primates, neurons that received stimulation from the central visual field were sensitive to images with a moving speed slower than 1 °/s, while those receiving stimulation from the peripheral

visual field preferred images with a moving speed faster than 30 °/s (Kelly, 1984; Orban et al., 1985). Yu et al. (2010) reported that the optimal speed of neurons in marmoset V1 increased significantly with eccentricity, with optimal speed values of 3.2 °/s, 6.7 °/s and 31.3 °/s for neurons with receptive fields in central, paracentral and peripheral visual fields, respectively. A similar result has been reported for marmoset area MT (Lui et al., 2007). In our study, the average optimal speed of V2 neurons receiving stimulation from the paracentral visual field was 17.44 °/s, which is significantly higher than the value of 6.7 °/s in the corresponding part of V1, and closer to observations in area MT. All of the above results indicate that the optimal speed of neurons in the visual cortex of primates increases with increasing eccentricity of the receptive field. Given the decrease in the optimal SF with increasing eccentricity, the increasing speeds allow constant TF selectivity.

Limitations, future directions and conclusions
Quantitative understanding of V2 response properties in the adult brain provides baseline measurements for future studies investigating the consequences of stroke and traumatic brain injury on the physiological processing of visual information (e.g. Hagan et al., 2017, 2020), and the effectiveness of regenerative therapies. The present results constitute a preliminary assessment of the responses of marmoset V2 neurons to gratings of varying SF and TF, but have some limitations that will require further studies. For example, the number of neurons that were subject to full study (110) was not sufficient to allow a full exploration of correlations between response properties. Hence questions such as the possible spatial clustering of cells with certain combinations of properties into V2 compartments (Levitt et al., 1994) or cortical layers will require additional experiments. Marmoset V2 has stripe-like compartments defined by cytochrome oxidase, similar to those observed in macaques (Roe et al., 2005; Jeffs et al., 2009), so clustering of response properties is to be expected. In addition, the present sample only consisted of neurons with receptive field eccentricities located in the paracentral visual field (8°–15°). For a more complete comparison with V1, a greater sample of receptive fields, ranging from central to far peripheral vision, is required. Other response properties, such as contrast sensitivity, should also be explored (Ghodrati et al., 2019). Finally, it would be useful to obtain simultaneous recordings from neurons in V1 and V2 with overlapping receptive fields, to test for temporal interactions between these two areas (e.g. Zavitz et al., 2019). The use of multielectrode arrays, which allow simultaneous recordings across borders of areas (Yu et al. 2020) will facilitate this endeavor. It is hypothesized that the responses of V2 neurons will be delayed relative to those of V1 neurons (Schmolesky et al., 1998). Looking further ahead, it would be desirable to correlate response properties to morphological properties of neurons, including the possibility that orientation selectivity is shaped by the morphology of dendritic trees (Elston and Rosa 1997, 1998).

In summary, we conclude that a large majority of neurons in marmoset V2 show sharp orientation selectivity, and that many (over a quarter) also show direction selectivity. According to the parameters tested, the responses of V2 cells closely resemble those observed in marmoset V1 (Yu et al., 2010), apart from the larger receptive field size (Rosa et al., 1997) and preferred speed. We found no bias in the distribution of preferred orientations, or evidence of SF-invariant speed selectivity. Despite the similarities between the characteristics of V1 and V2 neurons, studies in primates indicate that the main direction of information flow is from V1 to V2 because inactivation of V1 blocks most activity in V2 (Schiller and Malpeli, 1977; Girard and Bullier, 1989), which has implications for understanding the effects of occipital lobe lesions from stroke or trauma.

References

Baizer JS, Robinson DL, Dow BM (1977) Visual responses of area 18 neurons in awake, behaving monkey. J Neurophysiol 40:1024-1037.

Banks MS, Sekuler AB, Anderson SJ (1991) Peripheral spatial vision: limits imposed by optics, photoreceptors, and receptor pooling. J Opt Soc Am A 8:1775-1787.

Barraclough N, Tinsley C, Webb B, Vincent C, Derrington A (2006) Processing of first-order motion in marmoset visual cortex is influenced by second-order motion. Vis Neurosci 23:815-824.

Campbell FW, Kulikowski JJ (1966) Orientational selectivity of the human visual system. J Physiol 187:437-445.

Campbell FW, Cleland BG, Cooper GF, Enroth-Cugell C (1968) The angular selectivity of visual cortical cells to moving gratings. J Physiol 198:237-250.

Carandini M, Ferster D (2000) Membrane potential and firing rate in cat primary visual cortex. J Neurosci 20:470-484.

Cowey A (1964) Projection of the retina on to striate and prestriate cortex in the squirrel monkey, Saimiri Sciureus. J Neurophysiol 27:366-393.

De Valois RL, Yund EW, Hepler N (1982) The orientation and direction selectivity of cells in macaque visual cortex. Vision Res 22:531-544.

Eckert MP, Buchsbaum G (1993) Efficient coding of natural time varying images in the early visual system. Philos Trans R Soc Lond B Biol Sci 339:385-395.

Elston GN, Rosa MGP (1997) The occipitoparietal pathway of the macaque monkey: comparison of pyramidal cell morphology in layer III of functionally related cortical visual areas. Cereb Cortex 7: 432-452.

Elston GN, Rosa MGP (1998) Morphological variation of layer III pyramidal neurones in the occipitotemporal pathway of the macaque monkey visual cortex. Cereb Cortex 8: 278-294.

Foster KH, Gaska JP, Nagler M, Pollen DA (1985) Spatial and temporal frequency selectivity of neurones in visual cortical areas V1 and V2 of the macaque monkey. J Physiol 365:331-363.

Gattass R, Gross CG, Sandell JH (1981) Visual topography of V2 in the macaque. J Comp Neurol 201:519-539.

Ghodrati M, Zavitz E, Rosa MGP, Price NSC (2019) Contrast and luminance adaptation alter neuronal coding and perception of stimulus orientation. Nat Commun 10:941.

Girard P, Bullier J (1989) Visual activity in area V2 during reversible inactivation of area 17 in the macaque monkey. J Neurophysiol 62:1287-1302.

Gur M, Kagan I, Snodderly DM (2005) Orientation and direction selectivity of neurons in V1 of alert monkeys: functional relationships and laminar distributions. Cereb Cortex 15:1207-1221.

Hagan MA, Rosa MG, Lui LL (2017) Neural plasticity following lesions of the primate occipital lobe: The marmoset as an animal model for studies of blindsight. Dev Neurobiol 77:314-327.

Hagan MA, Chaplin TA, Huxlin KR, Rosa MGP, Lui LL (2020) Altered sensitivity to motion of area MT neurons following long-term V1 lesions. Cereb Cortex 30:451-464.

He LX, Wan L, Xiang W, Li JM, Pan AH, Lu DH (2020) Synaptic development of layer V pyramidal neurons in the prenatal human prefrontal neocortex: a Neurolucida-aided Golgi study. Neural Regen Res 15:1490-1495.

Henriksson L, Nurminen L, Hyvärinen A, Vanni S (2008) Spatial frequency tuning in human retinotopic visual areas. J Vis 8:5.1-13.

Henry GH, Bishop PO, Tupper RM, Dreher B (1973) Orientation specificity and response variability of cells in the striate cortex. Vision Res 13:1771-1779.

Hubel DH, Wiesel TN (1959) Receptive fields of single neurones in the cat's striate cortex. J Physiol 148:574-591.

Hubel DH, Wiesel TN (1962) Receptive fields, binocular interaction and functional architecture in the cat's visual cortex. J Physiol 160:106-154.

Hubel DH, Wiesel TN (1968) Receptive fields and functional architecture of monkey striate cortex. J Physiol 195:215-243.

Jeffs J, Ichida JM, Federer F, Angelucci A (2009) Anatomical evidence for classical and extra-classical receptive field completion across the discontinuous horizontal meridian representation of primate area V2. Cereb Cortex 19:963-981.

Kawabe T (2012) Postdictive modulation of visual orientation. PLoS One 7:e32608.

Kelly DH (1984) Retinal inhomogeneity. I. Spatiotemporal contrast sensitivity. J Opt Soc Am A 1:107-113.

Levitt JB, Kiper DC, Movshon JA (1994) Receptive fields and functional architecture of macaque V2. J Neurophysiol 71:2517-2542.

Liu C, Ye FQ, Newman JD, Szczupak D, Tian X, Yen CC, Majka P, Glen D, Rosa MGP, Leopold DA, Silva AC (2020) A resource for the detailed 3D mapping of white matter pathways in the marmoset brain. Nat Neurosci 23:271-280.

Lui LL, Bourne JA, Rosa MG (2005) Single-unit responses to kinetic stimuli in New World monkey area V2: physiological characteristics of cue-invariant neurones. Exp Brain Res 162:100-108.

Lui LL, Bourne JA, Rosa MG (2006) Functional response properties of neurons in the dorsomedial visual area of New World monkeys (Callithrix jacchus). Cereb Cortex 16:162-177.

Lui LL, Bourne JA, Rosa MG (2007) Spatial and temporal frequency selectivity of neurons in the middle temporal visual area of new world monkeys (Callithrix jacchus). Eur J Neurosci 25:1780-1792.

Majka P, Bai S, Bakola S, Bednarek S, Chan JM, Jermakow N, Passarelli L, Reser DH, Theodoni P, Worthy KH, Wang XJ, Wójcik DK, Mitra PP, Rosa MGP (2020) Open access resource for cellular-resolution analyses of corticocortical connectivity in the marmoset monkey. Nat Commun 11:1133.

Mansfield RJ (1974) Neural basis of orientation perception in primate vision. Science 186:1133-1135.

Mansfield RJ, Ronner SF (1978) Orientation anistropy in monkey visual cortex. Brain Res 149:229-234.

Mitchell DE, Freeman RD, Westheimer G (1967) Effect of orientation on the modulation sensitivity for interference fringes on the retina. J Opt Soc Am 57:246-249.

Movshon JA, Thompson ID, Tolhurst DJ (1978) Spatial and temporal contrast sensitivity of neurones in areas 17 and 18 of the cat's visual cortex. J Physiol 283:101-120.

Naito T, Okamoto M, Sadakane O, Shimegi S, Osaki H, Hara S, Kimura A, Ishikawa A, Suematsu N, Sato H (2013) Effects of stimulus spatial frequency, size, and luminance contrast on orientation tuning of neurons in the dorsal lateral geniculate nucleus of cat. Neurosci Res 77:143-154.

Nurminen L, Merlin S, Bijanzadeh M, Federer F, Angelucci A (2018) Top-down feedback controls spatial summation and response amplitude in primate visual cortex. Nat Commun 9:2281.

Olavarria JF, Van Essen DC (1997) The global pattern of cytochrome oxidase stripes in visual area V2 of the macaque monkey. Cereb Cortex 7:395-404.

Orban GA, Van Calenbergh F, De Bruyn B, Maes H (1985) Velocity discrimination in central and peripheral visual field. J Opt Soc Am A 2:1836-1847.

Osaki H, Naito T, Sadakane O, Okamoto M, Sato H (2011) Surround suppression by high spatial frequency stimuli in the cat primary visual cortex. Eur J Neurosci 33:923-932.

Patten ML, Mannion DJ, Clifford CWG (2017) Correlates of perceptual orientation biases in human primary visual cortex. J Neurosci 37:4744-4750.

Paxinos G, Watson C, Petrides M, Rosa MGP, Tokuno H (2012) The marmoset brain in stereotaxic coordinates. Cambridge, MA, USA: Academic Press.

Priebe NJ, Cassanello CR, Lisberger SG (2003) The neural representation of speed in macaque area MT/V5. J Neurosci 23:5650-5661.

Ringach DL, Shapley RM, Hawken MJ (2002) Orientation selectivity in macaque V1: diversity and laminar dependence. J Neurosci 22:5639-5651.

Roe AW, Fritsches K, Pettigrew JD (2005) Optical imaging of functional organization of V1 and V2 in marmoset visual cortex. Anat Rec A Discov Mol Cell Evol Biol 287:1213-1225.

Rosa MG, Sousa AP, Gattass R (1988) Representation of the visual field in the second visual area in the Cebus monkey. J Comp Neurol 275:326-345.

Rosa MG, Fritsches KA, Elston GN (1997) The second visual area in the marmoset monkey: visuotopic organisation, magnification factors, architectonical boundaries, and modularity. J Comp Neurol 387:547-567.

Rosa MG, Gattass R, Fiorani M, Jr., Soares JG (1992) Laminar, columnar and topographic aspects of ocular dominance in the primary visual cortex of Cebus monkeys. Exp Brain Res 88:249-264.

Rose D, Blakemore C (1974) An analysis of orientation selectivity in the cat's visual cortex. Exp Brain Res 20:1-17.

Schiller PH, Malpeli JG (1977) The effect of striate cortex cooling on area 18 cells in the monkey. Brain Res 126:366-369.

Schiller PH, Finlay BL, Volman SF (1976) Quantitative studies of single-cell properties in monkey striate cortex. II. Orientation specificity and ocular dominance. J Neurophysiol 39:1320-1333.

Schmolesky MT, Wang Y, Hanes DP, Thompson KG, Leutgeb S, Schall JD, Leventhal AG (1998) Signal timing across the macaque visual system. J Neurophysiol 79:3272-3278.

Sengpiel F, Troilo D, Kind PC, Graham B, Blakemore C (1996) Functional architecture of area 17 in normal and monocularly deprived marmosets (Callithrix jacchus). Vis Neurosci 13:145-160.

Sereno MI, Dale AM, Reppas JB, Kwong KK, Belliveau JW, Brady TJ, Rosen BR, Tootell RB (1995) Borders of multiple visual areas in humans revealed by functional magnetic resonance imaging. Science 268:889-893.

Snowden RJ, Hess RF (1992) Temporal frequency filters in the human peripheral visual field. Vision Res 32:61-72.

Solomon SG, Rosa MG (2014) A simpler primate brain: the visual system of the marmoset monkey. Front Neural Circuits 8:96.

Tao X, Zhang B, Smith EL, 3rd, Nishimoto S, Ohzawa I, Chino YM (2012) Local sensitivity to stimulus orientation and spatial frequency within the receptive fields of neurons in visual area 2 of macaque monkeys. J Neurophysiol 107:1094-1110.

Tolhurst DJ, Movshon JA (1975) Spatial and temporal contrast sensitivity of striate cortical neurones. Nature 257:674-675.
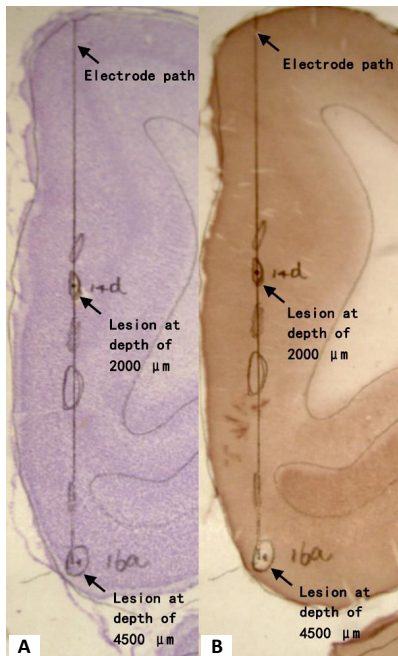
Figure 1 │ Example of a reconstructed electrode track, shown on 40 μm tissue sections stained for Nissl (A) and cytochrome oxidase (B).
This track crossed V2 along the midline wall (medial to the left), from the dorsal surface of the occipital lobe to the lip of the calcarine sulcus. The locations of electrolytic lesions used to identify cells recorded at specific depths are shown. The border between areas V1 and V2 is evident near the end of the tracks, with V1 showing a thick layer 4, densely stained for cytochrome oxidase (to the right of the reconstructed track). V1: The primary visual area (striate cortex); V2: the second visual area.
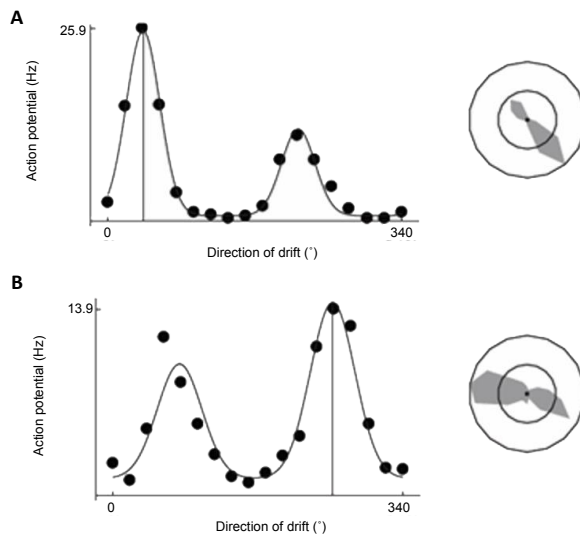
Figure 2 │ Tuning curves for different neurons in the second visual area of marmosets.
(A) A neuron with both orientation selectivity and direction selectivity. Left: Tuning curve of a neuron with both orientation selectivity and direction selectivity. The curve shows the average neuronal responses in action potentials as a function of the direction of drift of a grating (0–340°). Right: Same results displayed as a polar plot. In this representation, the outer circle corresponds to the maximal response, and the inner circle to the half-height response. For this cell: optimal direction = 40.5°, half-width-half-height bandwidth = 24.07, circular variance = 0.32, and DI2pt = 0.53. (B) A neuron with orientation selectivity but no direction selectivity. This cell had nearly equivalent responses to gratings drifting towards 257° and 84°, which correspond to an orientation of ~170°. Half-width-half-height bandwidth = 33.84, circular variance = 0.50, and DI2pt = 0.35. DI2pt: Direction index.
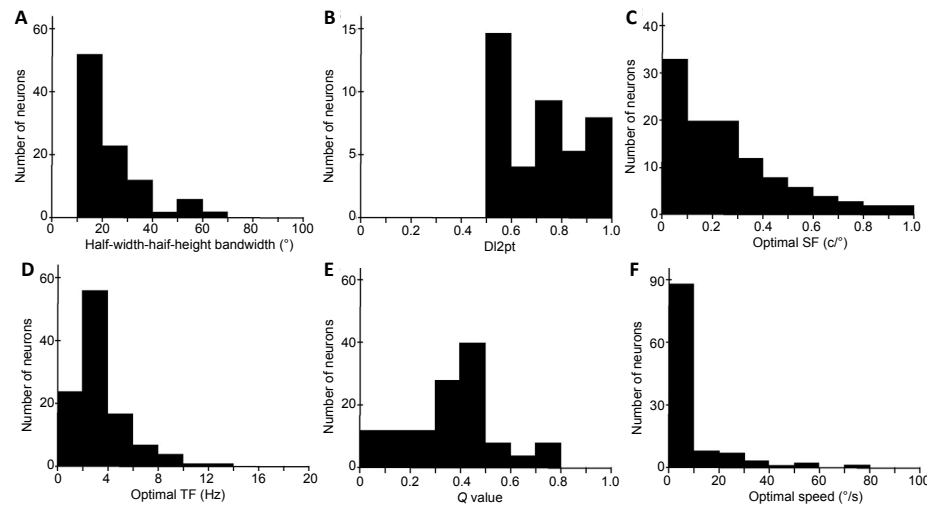
Figure 3 │ Visual response characteristics of neurons in the second visual area of marmosets
(A) Distribution of HWHH bandwidth among the 97 V2 neurons that were classified as orientation selective. (B) Distribution of DI2pt among the 31 neurons that were classified as direction selective. (C) Distribution of optimal SF values for 110 V2 neurons with receptive fields centered in the near periphery (8–15° eccentricity). (D) Distribution of optimal TF values for 110 V2 neurons. (E) Distribution of Q value among 31 direction-selective V2 neurons. (F) Distribution of optimal speed among 110 V2 neurons. DI2pt: Direction index; HWHH: half-width-half-height; SF: spatial frequency; TF: temporal frequency; V2: the second visual area.

Valverde Salzmann MF, Bartels A, Logothetis NK, Schüz A (2012) Color blobs in cortical areas V1 and V2 of the new world monkey Callithrix jacchus, revealed by non-differential optical imaging. J Neurosci 32:7881-7894.

Virsu V, Rovamo J (1979) Visual resolution, contrast sensitivity, and the cortical magnification factor. Exp Brain Res 37:475-494.

Virsu V, Rovamo J, Laurinen P, Näsänen R (1982) Temporal contrast sensitivity and cortical magnification. Vision Res 22:1211-1217.

Watkins DW, Berkley MA (1974) The orientation selectivity of single neurons in cat striate cortex. Exp Brain Res 19:433-446.

Worthy KH, Rosa MG (2017) Protocol for cytochrome oxidase histochemistry. http://r.marmosetbrain.org/CytochromeOxidase.pdf.

Worthy KH, Burman KJ (2017) Cresyl violet stain for nissl bodies. http://r.marmosetbrain.org/NisslStain.pdf.

Xu X, Anderson TJ, Casagrande VA (2007) How do functional maps in primary visual cortex vary with eccentricity? J Comp Neurol 501:741-755.

Yu HH, Rosa MG (2014) Uniformity and diversity of response properties of neurons in the primary visual cortex: selectivity for orientation, direction of motion, and stimulus size from center to far periphery. Vis Neurosci 31:85-98.

Yu HH, Chaplin TA, Rosa MG (2015) Representation of central and peripheral vision in the primate cerebral cortex: Insights from studies of the marmoset brain. Neurosci Res 93:47-61.

Yu HH, Verma R, Yang Y, Tibballs HA, Lui LL, Reser DH, Rosa MG (2010) Spatial and temporal frequency tuning in striate cortex: functional uniformity and specializations related to receptive field eccentricity. Eur J Neurosci 31:1043-1062.

Yu HH, Rowley DP, Price NSC, Rosa MGP, Zavitz E (2020) A twisted visual field map in the primate dorsomedial cortex predicted by topographic continuity. Sci Adv 6:eaaz8673.

Zavitz E, Yu HH, Rosa MG, Price NSC (2019) Correlated variability in the neurons with the strongest tuning improves direction coding. Cereb Cortex 29:615-626.

Zeki SM (1971) Cortical projections from two prestriate areas in the monkey. Brain Res 34:19-35.

Zeki SM (1978) Functional specialisation in the visual cortex of the rhesus monkey. Nature 274:423-428.

Zhao C, Hata R, Okamura JY, Wang G (2016) Differences in spatial and temporal frequency interactions between central and peripheral parts of the feline area 18. Eur J Neurosci 44:2635-2645.